Morphological Transitions in Model Membrane Systems by the Addition of Anesthetics

Magdalene Baciu,[†] Michael C. Holmes,* and Marc S. Leaver

Centre for Materials Science, Department of Physics, Astronomy, and Mathematics, University of Central Lancashire, Preston, PR1 2HE Lancashire, United Kingdom

Received: October 7, 2006; In Final Form: November 30, 2006

The mechanism of anesthetic action on membranes is still an open question, regardless of their extensive use in medical practice. It has been proposed that anesthetics may have the effect of promoting pore formation across membranes or at least switching transmembrane channels. In both cases this may be the result of changes in the interfacial curvature of the membrane due to the presence of anesthetic molecules. Aqueous solutions of surfactants display phases that mimic, in a simplified manner, real biological membranes. Therefore, in this study, two nonionic surfactant systems $C_{16}E_6/H_2O$ in concentrated solution and $C_{10}E_3/H_2O$ in dilute solution have been used as model membranes for the investigation of the effects of six common anesthetics (halothane, sodium thiopental, lidocaine base form and hydrochloride, prilocaine hydrochloride, and ketamine hydrochloride). Both binary surfactant−water systems exhibit phase transitions from the lamellar phase, L_α, that has zero spontaneous curvature and zero monolayer curvature to phases with more local interfacial curvature. These are the random mesh phase, $Mh_1(0)$, which consists of lamellae pierced by water-filled pores with local areas of positive interfacial curvature and the sponge phase, L_3, that consists of the lamellar phase with interlamellae attachments, often referred to as a "melted" cubic phase, possessing negative monolayer curvature. Small-angle X-ray scattering and ^2H NMR experiments upon the $C_{16}E_6/^2H_2O$ system and optical observations of the $C_{10}E_3/H_2O$ system showed that all anesthetics employed in this study cause a shift in the $Mh_1(0)$ to L_α phase transition temperature and in the L_α to L_3 transition temperature, respectively. All of the anesthetics studied bind to the interfacial region of the surfactant systems. Two types of behavior were observed on anesthetic addition: type I anesthetics, which decreased interfacial curvature, and type II, which increased it. However, at physiological pH both types of anesthetics decreased interfacial curvature.

1. Introduction

Anesthetics form a broad class of compounds with diverse molecular structures. Even though they have been in clinical use for well over 150 years, their site of action, lipid membrane or membrane proteins, remains an open question.[1]

Considering the lipid hypothesis of anesthesia, initial studies showed that clinical concentrations of anesthetics do not perturb significantly the structure of the lipid bilayer (i.e., dipalmitoylphosphatidylcholine, egg lecithin, dimyristoyl lecithin).[2,3] However, studies on model lipid bilayers have their limitations, even when the lipids used constitute the major component of real biological membranes. This is because real membranes are heterogeneous mixtures of lipids that can be saturated and unsaturated, charged or neutral, and in mixture with cholesterol and proteins that alone account for about 50% of the mass of the cell membrane. As a result, real membranes may not experience such sharp and defined phase transitions[1,4] as those in the model systems studied. In light of this, the hypothesis that lipids may play a significant role cannot be discounted.

Inhalation anesthetics have been shown to bind specifically to many proteins, for example, firefly luciferase,[5] serum albumin,[6] myoglobin,[7] and adenylate kinase,[8] and this has led to the protein hypothesis of anesthesia. However the fact that anesthetics do not induce tolerance (a characteristic of drugs acting on specific receptors) and their clinical concentrations are much higher (i.e., 10^3-10^6) than those of receptor-specific drugs indicates multiple molecular anesthetic targets.[1,9] Consequently a unified single model for the anesthetic action is elusive.

Thus the initial hypothesis that the site of anesthetic action involves the interface between the membrane proteins and the closely associated lipids[10,11] has been recently embraced with new interest regarding the role played by membrane lipids. It has been proposed that drugs may indirectly alter membrane protein function by modifying the membrane protein conformation[12−17] via lipid bilayer changes. This anesthetic action upon the lipid matrix indirectly triggering changes in protein conformation may be able to explain the reported effects of inhalation anesthetics upon ion channels,[18] since the hypothesis that the anesthetic acts exclusively on the $GABA_A$ receptor leads to a contradiction (i.e., anesthetic concentrations greater the 1 mM should lead to inhibition of the $GABA_A$ receptor, but this does not happen in practice, when higher anesthetic concentrations only deepen the anesthesia).[1,15]

Studies have shown, however, that one possible explanation for the action of anesthetic molecules is that they reside in the interfacial region of the membranes, promoting changes of the interfacial curvature.[19] Two broad classes of anesthetics have been identified as having an interfacial residence and a concomitant effect on the behavior of the system into which they are incorporated.[20] The first class is inhalation anesthetics, which are small, volatile molecules with an "amphiphilic" nature that possess a much higher solubility in oil than in water. It

* Author to whom correspondence should be addressed. E-mail: mcholmes@uclan.ac.uk.

[†] Current address: Institut für Physikalische Chemie I, Universität zu Köln, Luxemburger Strasse 116, D-50939 Köln, Germany.

10.1021/jp066595n CCC: $37.00
Published on Web 01/10/2007

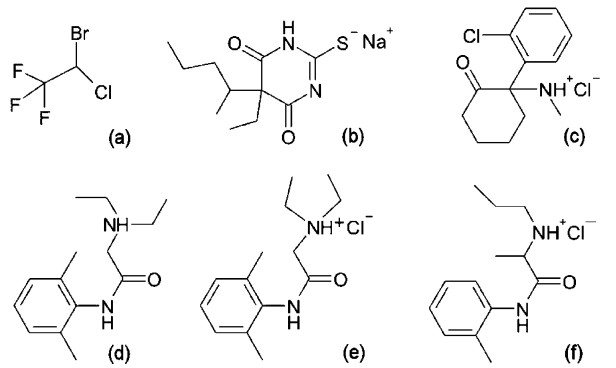

Figure 1. Structures of the anesthetic molecules used: (a) halothane, (b) sodium thiopental, (c) ketamine hydrochloride, (d) lidocaine base form, (e) lidocaine hydrochloride, and (f) prilocaine hydrochloride.

was proposed (i.e., Meyer−Overton correlation) that the anesthetic potency depends upon their partition coefficient between oil and water. However it is not sufficient for the anesthetic molecule to be only "hydrophobic".[21] Halothane (Figure 1a) is a widely used and potent inhalation anesthetic. It has an "acidic" proton that is responsible for the "hydrophilic" character, while the fluorinated carbon is responsible for its "hydrophobic" character. Thus, the halothane molecule resides in the interfacial region of a membrane.[20,22,23]

Local anesthetics are the second category of anesthetics that are proposed to reside at the interface between the membrane core and water.[20] Usually, they are part of the large cationic weakly amphiphilic drugs (CADs) family of molecules, and their effect is dependent upon both their hydrophobic and ionic character, for example, lidocaine base form (Figure 1d). They are used in base or acid form, and they are considered to either trigger lipid bilayer perturbations or have a specific effect upon membrane sodium channels.[23] The interfacial interaction of the above compounds has already been reported when added to a model membrane system.[24,25] The base form of lidocaine promotes phases with a higher curvature (i.e., reversed hexagonal phase, H_2), while the hydrochloride form favors flat interfaces (i.e., lamellar phase, L_α).

This interfacial residence may explain one of the commonly observed effects of anesthetics on membranes, namely, a leakage of one or more components through the membrane,[19,26] via the formation of membrane pores. However the detection of such pores is a difficult problem in real biological systems due to their complexity and to the high water content in the system. This results in phases that rarely possess long-range order, hence making routine structural investigations difficult.

There is a common aggregation process that causes the formation of both real and model membranes, and it is driven by the molecular amphiphilicity of the lipid and surfactant molecules in the system, respectively. Therefore, to look at the interaction of biologically relevant additives, alternative, less complex, amphiphilic, self-assembling systems have been used as test systems. Lamellar or vesicular phases formed in surfactant or simplified lipid systems are the most regularly utilized.[23] The phases that occur in surfactant/water systems and in lipid/water systems are stable for given sets of conditions, i.e., temperature, concentration, and intra- and interaggregate interactions.[27] Perturbation of these conditions leads to alterations in the interfacial curvature with the concomitant possibility of changing the phase structure of the self-assembled phase. Therefore the interfacial curvature has an important role in controlling phase structure and its resultant stability. Indeed although real biological membranes are usually "flat" structures on a micron length scale, at a molecular level their stability is increased by adopting a certain degree of curvature,[28] again indicating the importance of interfacial curvature in membrane systems.[25] Since it is proposed that anesthetics reside in the interfacial region of membranes,[20,23] it can be expected that their effect on surfactant/water systems will be to alter the interfacial curvature and hence their phase structures, providing an ideal route for a better understanding of the possible molecular mechanisms of anesthetic−membrane interactions.

The formation of pores in surfactant/water lyotropic lamellar phases has been shown to be a result of small perturbations of the surface packing within the phase.[29−31] However the formation of pores is not straightforward to detect. In a porous lamellar phase or random mesh phase, the overall symmetry of the phase is maintained; however the bilayer is pierced by water-filled defects, whose presence can be inferred only by correlating the results from a series of techniques such as NMR, optical microscopy, and small-angle X-ray scattering (SAXS).[29,32] It has been possible to show that pore formation in surfactant systems is a direct result of a slight increase in the surface area occupied by each surfactant molecule at the interface. This increase can be driven by a change in the hydration of the head groups or an alteration in the intraaggregate interactions in nonionic and ionic surfactant systems, respectively. Some examples of structures with pore or bicontinuous structures are shown in ref 33.

In the present work, we have investigated the effects of anesthetic addition upon two surfactant/water systems that offer the unique possibility of determining whether pore formation is a consequence of anesthetic addition to membrane-like systems and to study the effect of anesthetics upon phases that possess nonuniform interfacial curvature: mesh phase $Mh_1(0)$ in $C_{16}E_6/H_2O$ and L_3 sponge phase in $C_{10}E_3/H_2O$. Phases with nonuniform interfacial curvature are likely to occur in real biological membranes, because of their heterogeneous lipid composition.

The $Mh_1(0)$ phase and L_3 sponge phase exhibit increased interfacial monolayer curvature (either positive or negative, respectively). The systems chosen for study were the commercially available nonionic surfactants $C_{16}E_6/H_2O$[29,34,35] and $C_{10}E_3/H_2O$.[36] $C_{16}E_6/H_2O$ was studied at high surfactant concentrations where the lamellar phase, L_α, to $Mh_1(0)$ phase transition occurs, and the $C_{10}E_3/H_2O$ system was studied in dilute solution as well as in buffered solution where the L_α to L_3 transition occurs. The phase diagram of the nonionic surfactant $C_{10}E_3$ when mixed with water displays a range of liquid crystalline phases, but the dominant phase is L_α.[36] At low surfactant concentrations it is possible to form the L_3 phase. This phase can be thought of as a multiply connected lamellar phase or "melted" cubic phase or a sponge phase having a structural bilayer unit identical with the lamellar phase, L_α, but possessing inter-bilayer connectivity and a significantly different topology.[37] The transition between the L_α and the L_3 phases is therefore subtle and driven by topological reorganizations in an environment where inter-bilayer interactions can be negligible. A comparative study with short-chain oil (i.e., octane) and alcohol (i.e., octanol) on the same model system were also undertaken as control experiments. Both octane and octanol are known to affect nonionic surfactant self-assembly and are well-studied and understood.

2. Experimental Section

2.1. Materials. The surfactants used were the nonionic surfactants hexaethylene glycol mono-*n*-hexadecyl ether ($C_{16}E_6$,

$M_w = 506.86$) and triethylene glycol mono-*n*-decyl ether ($C_{10}E_3$, $M_w = 290.5$). Both were purchased from Nikko Chemicals Co. (Tokyo, Japan) and were ≥99% pure.

The solvents used were Millipore filtered water with a low ion concentration and deuterium oxide. Deuterium oxide (^2H_2O, $M_w = 20.03$) was purchased from Sigma Chemicals (Gillingham, U. K.) for the experiments with concentrated surfactant/water systems, or it was obtained from Dr. Glaser AG (Basel, Switzerland) for the experiments performed in dilute regions of surfactant/water systems. In both cases the ^2H_2O had a purity of ≥99.8%.

The inhalation anesthetic halothane (i.e., 2-bromo-2-chloro-1,1,1-trifluoroethane), with a >99% purity, was purchased from Sigma Chemicals (Gillingham, U. K.) ($M_w = 197.4$, $\rho = 1.88$ g/mL). The intravenous general anesthetic agents the barbiturate sodium thiopental (i.e., 5-ethyl-5-[1-methylbutyl]-2-thiobarbituric acid sodium salt/sodium carbonate mixture, $M_w = 264.3$) and ketamine hydrochloride (i.e., 2-[2-chlorophenyl]-2-[methylamino]-cyclohexanone hydrochloride, $M_w = 273.37$) were purchased from Sigma Chemicals (Gillingham, U. K.). Both have a purity of ≥98%. Local anesthetics lidocaine (i.e., 2-diethylamino-*N*-[2,6-dimethylphenyl]acetamide, lignocaine or xylocaine) in its two forms lidocaine base form ($M_w = 234.34$) and lidocaine hydrochloride ($M_w = 270.8$) and prilocaine hydrochloride (i.e., *N*-[2-methylphenyl]-2-[propylamino]-propamide, $M_w = 256.8$), all with >98% purity, were purchased from Sigma Chemicals (Gillingham, U. K.).

The oil *n*-octane (>99% pure) was purchased from Lancaster Chemicals (Lancaster, U. K.), while the alcohol octan-1-ol was purchased from Merck (West Drayton, U. K.). The oil *n*-heptane (>99% pure) was obtained from Sigma Chemicals (Gillingham, U. K.). NaCl (sodium chloride, $M_w = 58.44$), Na_2HPO_4 (disodium hydrogen orthophosphate anhydrous, $M_w = 141.96$), and KH_2PO_4 (potassium dihydrogen orthophosphate, $M_w = 136.09$), all with > 99% purity, used to produce a 0.1 M phosphate-buffered saline (PBS) solution, were purchased from Merck (West Drayton, U. K.).

All of the chemicals involved in this study were used as purchased without further purification.

2.2. Sample Preparation. *2.2.1. Binary Samples.* Binary surfactant system samples were prepared by weighing the required amounts of surfactant and water or ^2H_2O into the glass sample tube, which had a constriction at the middle to aid mixing. After the surfactant and water or ^2H_2O were added, the sample tubes were sealed with Parafilm and centrifuged to ensure that all sample components are at the base of the sample tube prior to flame sealing.

For the nonionic surfactant $C_{16}E_6$ the binary samples were prepared at room temperature, but during mixing the temperature was raised above 31 °C to prevent phase separation that occurs below this temperature. Sample homogenization was achieved by repeated centrifugation and then by keeping them for a time between 6 and 30 h in the oven at 50 °C (a temperature at which the system exhibits the lamellar phase).

The nonionic $C_{10}E_3$ surfactant binary samples were prepared in glass tubes with screw caps, at room temperature. The homogenization was achieved by vortex mixing at room temperature, and their bulk optical texture was checked with the naked eye and between cross-polarizers.

2.2.2. Ternary Samples. The ternary system samples consist of surfactant, anesthetic, and solvent (i.e., water, ^2H_2O, or 0.1 M PBS). The mole ratio of surfactant to ^2H_2O was fixed to (i) 0.046 corresponding to a 54 wt % $C_{16}E_6/^2H_2O$ binary system, (ii) 0.004 corresponding to a 5 wt % $C_{10}E_3/^2H_2O$ binary system, and (iii) 0.003 corresponding to a 5 wt % $C_{10}E_3/H_2O$ binary system.

For all of the samples the mole ratio of anesthetic to surfactant was calculated from $n_s/n_a = (M_a/M_s) \times ((100 - x)/x) \times (c/100)$ where n_s and n_a are the number of moles of surfactant and anesthetic, M_s and M_a are the molar masses of surfactant and anesthetic, respectively, c is the binary surfactant concentration (wt %) in the surfactant solvent mixture, and x is the anesthetic concentration (wt %) in the ternary sample.

Microslides (0.2 mm path length flat capillaries) were filled from the sample tube for optical microscopy. For NMR and SAXS experiments 5 mm NMR tubes and, 0.5, 0.7, or 1.0 mm Lindeman capillaries, respectively, were filled. However, in the case of the volatile anesthetic, halothane, NMR samples were prepared directly in the NMR tubes to minimize the risk of loss of anesthetic by evaporation. After being filled, the tubes were flame-sealed, and the liquid level was marked. Its integrity was tested by leaving it overnight in the oven at 50 °C.

2.3. Experimental Techniques. *2.3.1. Nuclear Magnetic Resonance.* For NMR experiments a Bruker Advance DPX250 NMR spectrometer was used, operating at 38.3 MHz for ^2H and controlled using XWIN NMR version 1.1. A sample equilibration time of 30 min was allowed after each temperature change.

In systems containing nonionic surfactants Rendall et al.[38,39] showed that the ^2H NMR quadrupolar splitting ($\Delta\nu$) obtained from ^2H_2O bound to the first one or two ethylene oxide groups of the surfactant molecule can be expressed as

$$\Delta\nu = \frac{1}{2}\Delta\nu_0 p_b S_b \qquad (1)$$

where p_b is the fraction of bound ^2H_2O molecules, S_b is the orientational order parameter of the bound water, and $\Delta\nu_o$ is the splitting associated with a bound ^2H_2O molecule. In the binary system the variation of the quadrupolar splitting as a function of temperature and surfactant concentration helps to delineate the phase transitions and distinguishes between single and coexisting phases.[34] Samples show Pake powder patterns indicating no particular orientations of the phases; splittings were measured from the inner two peaks, $\Delta\nu$.

2.3.2. Small-Angle X-ray Scattering. SAXS experiments have been performed in the laboratory at Preston, at Daresbury SRS Laboratory station 6.1, Warrington, and at Desy HASYLAB, Hamburg, Germany.

For the experiments performed at Daresbury the camera was calibrated using rat tail collagen. Samples were held in a Linkham THM 600 sample stage with the temperature controlled by a Linkham TMS 19, to an accuracy of ±0.1 °C. At Desy HASYLAB the experiments were performed on beam line A2. The camera was calibrated using silver behenate. Two Eurotherm dual-loop controllers (EPC 905 D) were used to control the temperature (±0.1 °C).

2.3.3. Water Bath Experiments. A Lauda 200 water bath with a temperature control device (±0.1 °C) was used. After preparation the samples were submerged in the water bath where they were left to achieve complete equilibration. The experiments consisted of the visual observation of the sample bulk texture using cross-polarizers, while the temperature was varied stepwise between 18 and 40 °C, with steps of 0.5 °C for the $C_{10}E_3/^2H_2O$ system and 0.1 °C for the $C_{10}E_3$/0.1 M PBS system. The sample temperature was allowed 15−20 min to equilibrate. This equilibration time was decided upon, since in this system the kinetics are known to be fast.

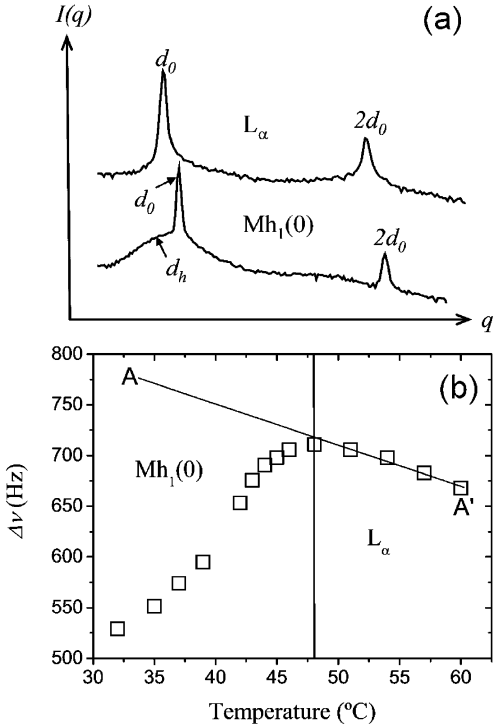

Figure 2. (a) Small-angle X-ray scattering from a 54% by weight $C_{16}E_6/^2H_2O$ sample in the L_α and $Mh_1(0)$ phases. Note in the latter the appearance of a broad peak, d_h, which is the diffuse scattering from the in-plane water-filled pores. (b) ^2H NMR splitting $\Delta\nu$ taken from the inner peaks of the spectrum and measured from a 54% by weight $C_{16}E_6/^2H_2O$ sample as a function of temperature. The vertical line shows the position of the L_α to $Mh_1(0)$ phase transition. The line AA′ shows the extrapolation of the L_α phase behavior back to low temperatures.

3. Results

3.1. $C_{16}E_6/^2H_2O$ System. The lamellar and random mesh phases exhibited by a 54 wt % $C_{16}E_6/^2H_2O$ sample were examined in the presence of halothane, sodium thiopental, ketamine hydrochloride, lidocaine (base and hydrochloride forms), and prilocaine hydrochloride.

The formation of a random mesh phase out of a classical lamellar phase has been well-documented in this binary surfactant water system.[27,34,40,41] Figure 2a shows the SAXS from the classical lamellar, L_α, and random mesh, $Mh_1(0)$, phases. In both cases the scattering is dominated by strong first- and second-order reflections in a ratio of 1:2, characteristic of a classical lamellar phase. However in the $Mh_1(0)$ phase the separation of the layers is significantly reduced due to the incorporation of water into pores within the lamellae. In addition, in the $Mh_1(0)$ phase a third diffuse scattering feature labeled d_h in Figure 2a is observed, which arises from the scatter from the water-filled pores and gives a measure of the mean center-to-center distance of the pores with the layers. The appearance of this feature and the narrowing of the layer spacing with decreasing temperature are coincident with a "turnover" in the temperature evolution of the ^2H NMR quadrupolar splitting ($\Delta\nu$) (Figure 2b).

3.1.1. ^2H NMR. The formation of the pores within the bilayers is associated with an increase in the interfacial curvature reflected by a decrease in $\Delta\nu$. The turnover of $\Delta\nu$ can be used as a marker for the $Mh_1(0)$ to L_α phase transition at temperature T_C.[32,34] Figures 3 and 4 show the effect of the anesthetics on the evolution of $\Delta\nu$ as a function of temperature and anesthetic concentration for a 54 wt % sample of $C_{16}E_6/^2H_2O$. The first obvious feature is that the evolution of $\Delta\nu$ with temperature

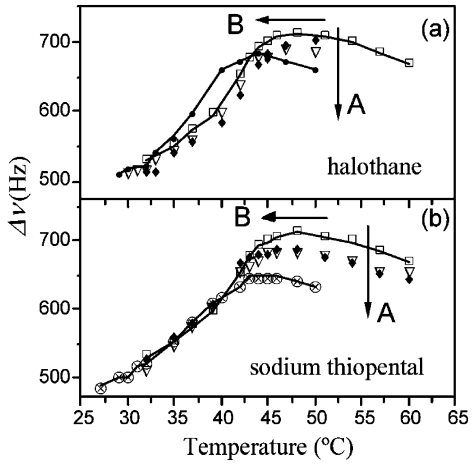

Figure 3. $\Delta\nu$ vs temperature for a 54% by weight $C_{16}E_6/^2H_2O$ sample with various amounts of added type I anesthetic. Symbols represent the mole ratio of anesthetic to surfactant: 0 (□), 0.04 (◆), 0.07 (▽), 0.11 (⊗), and 0.23 (●). Experimental errors are approximately 3%, but error bars have been omitted for clarity. Lines are a guide to the eye and have been included for 0% and 5% by weight halothane in part a and 0% and 3% by weight sodium thiopental in part b. The arrows labeled A indicate the change in $\Delta\nu$ in the L_α phase, while arrows labeled B indicate the direction of the shift in the L_α to $Mh_1(0)$ phase transition.

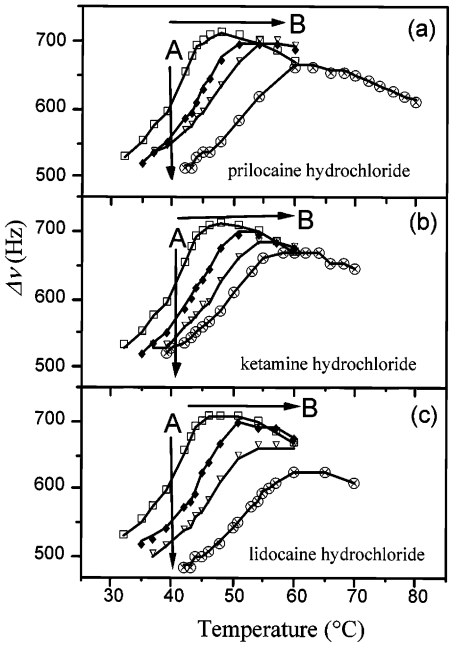

Figure 4. $\Delta\nu$ vs temperature for a 54% by weight $C_{16}E_6/^2H_2O$ sample with various amounts of added type II anesthetic. Experimental errors and symbols are as in Figure 3. Lines are a guide to the eye. The arrows labeled A indicate the change in $\Delta\nu$ in the $Mh_1(0)$ phase, while arrows labeled B indicate the direction of the shift in the L_α to $Mh_1(0)$ phase transition.

follows the same pattern as in the binary system, although there are shifts in T_C and decreases in $\Delta\nu$ values, which depend upon the type of anesthetic and its concentration. The direction in which the anesthetic addition shifts the phase transition temperature divides them into two groups, which will be referred to as type I (Figure 3) and type II (Figure 4).

Type I anesthetics (Figure 3) consist of the general anesthetic halothane, the barbiturate sodium thiopental, and the local anesthetic lidocaine as its base form. Within the L_α phase these anesthetics promote a drop in $\Delta\nu$ but only a marginal shift in

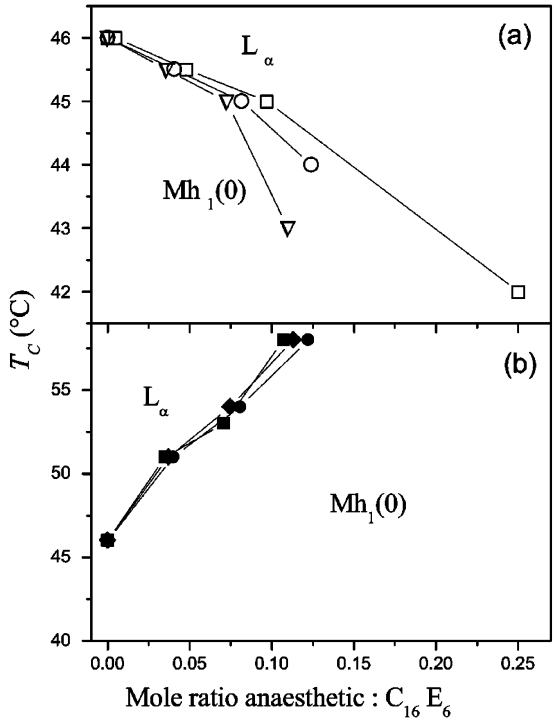

Figure 5. L_α to $Mh_1(0)$ phase transition temperature, T_C as a function of anesthetic to $C_{16}E_6$ mole ratio. Lines are a guide to the eye. (a) Type I anesthetics: halothane (□), sodium thiopental (○), and lidocaine base (▽). (b) Type II anesthetics: lidocaine hydrochloride (■), prilocaine hydrochloride (◆), and ketamine hydrochloride (●).

T_C to a lower temperature. The $Mh_1(0)$ phase is almost unaffected by the anesthetic addition.

Type II anesthetics (Figure 4) consist of the local anesthetics lidocaine hydrochloride and prilocaine hydrochloride and the dissociative agent ketamine hydrochloride. In the L_α phase $\Delta\nu$ is hardly changed by these anesthetics, but they do shift T_C to a higher temperature by as much as 14 °C. Thus they favor the presence of random mesh phase, $Mh_1(0)$, at a higher temperature with respect to the binary system. Within the $Mh_1(0)$ phase, $\Delta\nu$ evolution is strongly dependent upon anesthetic concentration.

Within the 54 wt % $C_{16}E_6/^2H_2O$ system the thermal evolution of $\Delta\nu$ during the phase transition is related to the evolution of curvature in the system. Therefore changes in the phase transition boundary imply changes in interfacial curvature triggered by anesthetic addition. The change in the phase boundary of type I and II anesthetics are shown in Figures 5a and 5b, respectively.

3.1.2. Small-Angle X-ray Scattering-. SAXS spectra were recorded for all of the type I and II anesthetics on cooling usually from the L_α to the $Mh_1(0)$ phase for anesthetic to surfactant mole ratios of 0.04, 0.07, and 0.11. For all samples studied the transition between these phases is marked by a decrease in the layer separation and the appearance of the diffuse scattering feature associated with d_h. No new scattering features were observed at any anesthetic concentration studied irrespective of the anesthetic type.

Figure 6 shows a typical example from the 54 wt % $C_{16}E_6/^2H_2O$ system with lidocaine hydrochloride (mole ratio of 0.11). NMR from this sample shows that the transition from the L_α to the $Mh_1(0)$ phase occurs at ~52 °C, which SAXS results support with the appearance of a diffuse scatter feature under the first-order peak and a decrease in the layer spacing at 50 °C. These features become more pronounced as the temperature decreases.

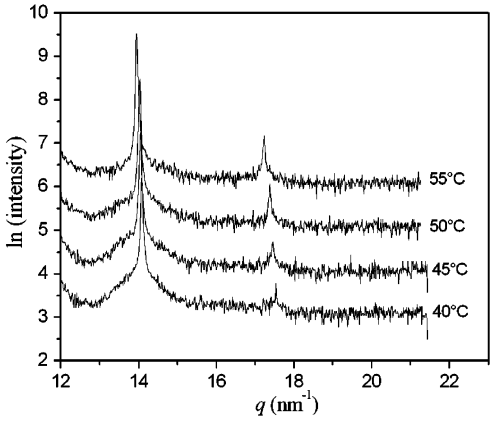

Figure 6. SAXS as a function of temperature, observed for a typical sample of 54 wt % $C_{16}E_6/^2H_2O$ system with lidocaine hydrochloride (mole ratio of 9:1).

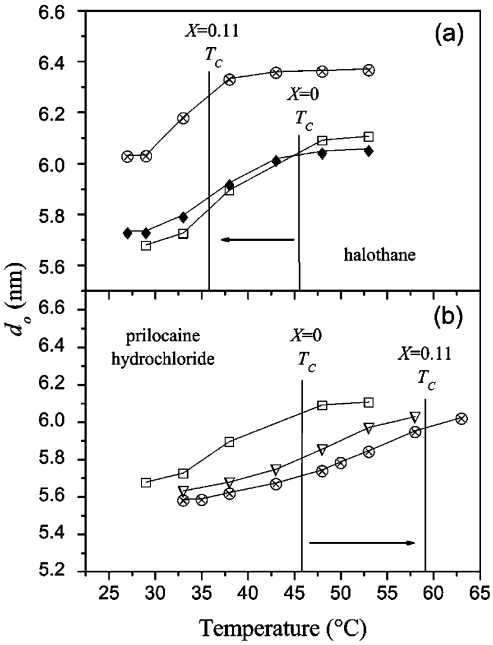

Figure 7. Layer spacing, d_0, plotted as a function of temperature for (a) a type I anesthetic (halothane) and (b) a type II anethetic (prilocaine hydrochloride). Symbols represent the mole ratio of anesthetic to surfactant, X: 0 (□), 0.04 (◆), 0.07 (▽), and 0.11 (⊗). T_C values for the 0 and 0.11 mole ratio of anesthetic are marked by vertical lines. The arrows indicated the change in T_C with increasing anesthetic concentration. The lines between the points are a guide to the eye.

The effect of the type I anesthetic is to increase the position of the first-order peak, with the increase being most marked for the largest amount of added anesthetic (Figure 7a). Coupled with this increase of ~0.4 nm is a shift to lower temperatures of the point at which the layer separation begins to decrease and the d_h reflection is observed, which is consistent with the NMR observation of a shift of T_C to a lower temperature.

For the type II anesthetic there is almost no effect on the position of the first-order peak at high or low temperature, irrespective of the amount of anesthetic added. However the point at which the layer separation begins to decrease and the d_h reflection is observed occurs at higher temperatures, which is consistent with the NMR observation of a shift of T_C to a higher temperature (Figure 7b).

3.2. $C_{10}E_3$ System. Visual observations in a water bath were made of the effects of anesthetics upon the L_α to ($L_\alpha + L_3$), ($L_\alpha + L_3$) to L_3, and L_3 to ($L_3 + W$) transition temperatures of the 5 wt % $C_{10}E_3/^2H_2O$ binary system. In fact all three transitions

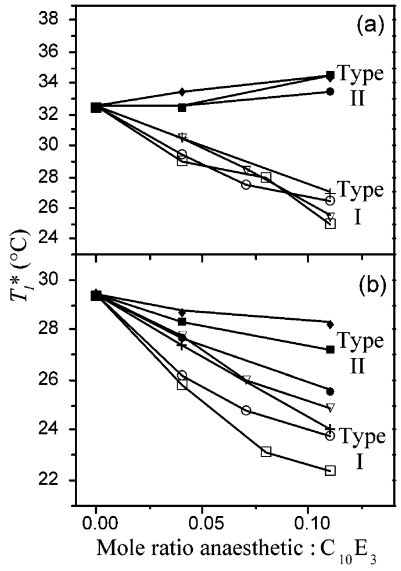

Figure 8. Variation of the L_α to $L_\alpha + L_3$ transition temperature, T_1^*, with anesthetic concentration, (a) 5% by weight $C_{10}E_3/H_2O$ system and (b) 5% by weight $C_{10}E_3$/0.1 M PBS system, pH = 7.4. Lines are a guide to the eye. (a) Type I anesthetics: halothane (□), sodium thiopental (○), and lidocaine base (▽). (b) Type II anesthetics: lidocaine hydrochloride (■), prilocaine hydrochloride (◆), and ketamine hydrochloride (●). Octanol is represented by "+".

behaved identically for all eight additives, and consequently only the L_α to ($L_\alpha + L_3$) transition will be used as an example. The behavior can be classified into the same two types previously observed in the $C_{16}E_6/^2H_2O$ system. In addition, as controls, octane and octanol addition were investigated, and it was found that both behave like type I anesthetics.

3.2.1. Type I Anesthetics, Oil, and Alcohol. Halothane, sodium thiopental, and the lidocaine base form, together with the short-chain oil and alcohol, cause a decrease in the phase transition temperatures by as much as 7 °C, Figure 8a, that is concentration-dependent.

3.2.2. Type II Anesthetics. Lidocaine hydrochloride, prilocaine hydrochloride, and ketamine hydrochloride cause a smaller increase (1.5−2 °C) in all transition temperatures with respect to the binary system (Figure 8a).

The effect upon the phase transition temperature caused by the type II anesthetics is about 4 times weaker than the effect of type I anesthetics. These results in a dilute surfactant system may be contrasted with those obtained in the concentrated $C_{16}E_6/^2H_2O$ system. Type I anesthetics lower transition temperatures in both concentrated and dilute systems although the effect is larger in the dilute system. In contrast type II anesthetics increase the transition temperatures although the effect is much larger in the concentrated system (cf. Figures 8a and 5).

3.2.3. Anesthetics, Oil, and Alcohol Addition in Buffered Solution. To approach a more realistic solution environment, the dilute region of the nonionic surfactant $C_{10}E_3$/water system was buffered to the physiological value of pH = 7.4, using a 0.1 M PBS solution. Buffering the pH caused a decrease of all of the phase transition temperatures by 3 °C within the $C_{10}E_3/H_2O$ binary system. The results show clearly that the addition of all anesthetics, oil, and alcohol decrease the phase transition temperature between the L_α and the L_3 phases (Figure 8b and Table 1). Thus all anesthetics together with the short-chain oil and alcohol behave more like type I anesthetics when pH is buffered to the physiological value of 7.4, within the $C_{10}E_3$/PBS 0.1M system, causing a lowering of phase transition temperatures with increasing additive concentrations.

4. Discussion

4.1. $C_{16}E_6/^2H_2O$ System. Equation 1 shows that $\Delta\nu$ is proportional to both the hydration of the head group, i.e., the fraction of bound water, p_b, and the order parameter of the bound water, S_b. In a nonionic surfactant water system, in the L_α phase, $\Delta\nu$ increases slowly with decreasing temperature, reflecting an increase in water hydration, p_b, and changes in the order parameter, S_b, of the bound water. It is well-established that the hydration of the head groups, p_b, of these nonionic surfactants increases with decreasing temperature.[42]

The effects of type I and II anesthetics on the L_α phase at a fixed temperature can now be contrasted. The addition of type I anesthetics (Figure 3) promote a drop in $\Delta\nu$ while type II anesthetics (Figure 4) hardly change $\Delta\nu$ at all. Evidence shows that anesthetic molecules bind to the interfacial region with their hydrophobic moieties being associated with the α-CH_2 group.[20,23] Type I anesthetics also possess a polar moiety that displaces water from between the ethylene oxide head groups, enhancing their dehydration and decreasing $\Delta\nu$.

The effects of changes in hydration of the ethylene oxide head groups either through changes in temperature or by binding of anesthetic molecules can be eliminated to expose the ability of anesthetics to promote increased surface curvature in the form of water-filled pores. $\Delta\nu$ in the L_α phase is denoted by $\Delta\nu^{L_\alpha}$ and can be projected back to low temperatures (see line AA′ in Figure 2b as an example). A curvature formation parameter,[32] σ, may be calculated by forming the ratio $\Delta\nu/\Delta\nu^{L_\alpha} = \sigma$. In the L_α phase $\sigma = 1$, but within the $Mh_1(0)$ phase $^1/_2 \leq \sigma \leq 1$. The lower the value of σ, the higher the average interfacial curvature, and the more curved the edges. Here interfacial curvature is the mean curvature, $H = (^1/_2)(1/r_1 + 1/r_2)$ where r_1 and r_2 are the radii of curvature of two orthogonal arcs intersecting at a point on the surface.

4.1.1. Type I Anesthetics. σ is plotted in Figure 9a for halothane, as an example of type I behavior, as a function of temperature, anesthetic type, and concentration. Within the $Mh_1(0)$ phase, σ increases as the concentration of the anesthetic increases and shows that the addition of type I anesthetics reduces the interfacial curvature, altering the stability of pores in the $Mh_1(0)$ phase. Type I anesthetics promote flatter interfaces and reduce the occurrence of water-filled pores.

Type I anesthetics are polar, and they simply displace water from the first ethylene oxide group region, increasing the dehydration. Hence type I anesthetics have the same effect as increasing the temperature: They promote the dehydration of the ethylene oxide head groups, allowing them to pack closer together. This causes a decrease of the amount of curvature in the system, and consequently the $Mh_1(0)$ to L_α phase transition moves to a lower temperature (Figure 5a).

4.1.2. Type II Anesthetics. Figure 9b for prilocaine hydrochloride, chosen as an example of a type II anesthetic, shows the variation of σ with temperature and anesthetic concentration. Within the $Mh_1(0)$ phase, σ decreases as the concentration of anesthetic increases. Type II anesthetics promote greater interfacial curvature and increase the occurrence of water-filled pores.

Type II anesthetics carry a localized charge in their molecules. The association of the charged part of their molecule with the base of the head group region may affect the interfacial curvature. Charvolin et al.[43] showed using contrast variation neutron scattering that alcohol added to sodium dodecyl sulfate/^2H_2O is preferentially localized at the highly curved edges found in that system. In other words, the alcohol is inhomogeneously

TABLE 1: Anesthetic Addition to $C_{10}E_3$/0.1 M PBS System

			$C_{10}E_3$/0.1 M PBS (pH = 7.4)		
	anesthetic	mole ratio (anesthetic to $C_{10}E_3$)	T_1^* (°C)	T_2^* (°C)	T_3^* (°C)
1	halothane	0.04	−3.6	−3.7	−4
		0.07	−6.3	−6.5	−6.4
		0.11	−7	−6.9	−7.2
2	thiopental sodium	0.04	−3.2	−3.2	−4.1
		0.07	−4.6	−5.3	−5.7
		0.11	−5.6	−6.5	−6.9
3	lidocaine base	0.04	−1.6	−1.6	−1.8
		0.07	−3.4	−3.6	−4
		0.11	−4.5	−4.9	−5
4	lidocaine hydrochloride	0.04	−1.1	−1.2	−1.4
		0.11	−2.2	−2.4	−2.5
5	priolocaine hydrochloride	0.04	−0.6	−0.8	−0.7
		0.11	−1.1	−1.3	−1.5
6	ketamine hydrochloride	0.04	−1.7	−1.7	−1.9
		0.11	−3.8	−4	−4.3
7	octanol (alcohol)	0.04	−2	−1.7	−2.1
		0.11	−5.4	−5.1	−5.7
8	octane (oil)	0.04	−1.8	−1.6	−2.1
		0.11	−5.1	−4.9	−5.5

[a] Note that T_1^*, T_2^*, and T_3^* represent the transition temperatures from L_α to $L_\alpha + L_3$, $L_\alpha + L_3$ to L_3, and L_3 to $L_3 + W$, respectively. For all of the experiments a temperature step of 0.1 °C was used.

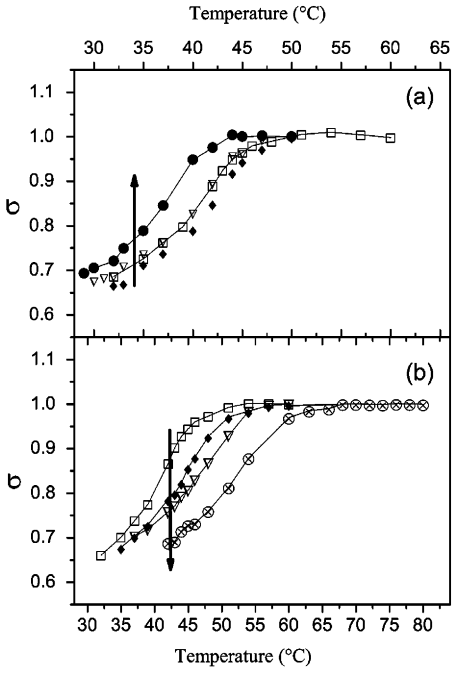

Figure 9. Curvature formation parameter, σ, plotted as a function of temperature and anesthetic concentration for (a) a type I anesthetic (halothane) and (b) a type II anesthetic (prilocaine hydrochloride). The vertical arrows indicate the direction of change in σ as the anesthetic concentration is increased. Solid lines are a guide to the eye. Symbols have the same meaning as in Figure 3.

distributed and stabilizes the development of structures with nonuniform interfacial curvature.

In the $C_{16}E_6/^2H_2O$ system, in the $Mh_1(0)$ phase, the interfacial curvature is nonuniform, being greater around the water-filled pores. Type II anesthetics are charged and may be located on the highly curved edges where there is a higher degree of separation of the ethylene oxide head groups, minimizing the repulsive interactions of the type II anesthetic charged groups. Thus they will charge up the edges, introducing electrostatic repulsion and stabilizing the pores. Hence the $Mh_1(0)$ phase is stabilized to a higher temperature (Figure 5b).

There is some evidence from work on nerve membranes[44−47] for this difference in behavior of the two types of anesthetics. It has been claimed that, at least for local anesthetics, the protonated form (e.g., lidocaine hydrochloride, type II) does not penetrate the membrane, while the unprotonated form (e.g., lidocaine base, type I) is able to penetrate the membrane. Type I anesthetics will therefore be more easily solubilized in the hydrophobic core and behave in a similar way to added oil, encouraging the loss of curvature and the formation of the lamellar phase. In contrast, type II anesthetics will tend to remain anchored to the interface and may help to stabilize the curvature.

In summary, both types of anesthetics bind at the interfacial region. Type I anesthetics dehydrate the ethylene oxide head groups and reduce the interfacial curvature, while type II anesthetics carry a localized charge and probably microsegregate onto the curved pore edges, stabilizing the $Mh_1(0)$ phase to a higher temperature.

4.2. $C_{10}E_3$ System. The effect on the L_α to L_3 phase transition temperature divides the anesthetics into the same two types as in the concentrated system $C_{16}E_6/^2H_2O$.

4.2.1. Type I Anesthetics. Increasing the concentration of type I anesthetic, oil and alcohol cause a decrease in the transition temperature from the L_α to the L_3 phase in the 5 wt % $C_{10}E_3/^2H_2O$ system. However, the effect of type I anesthetics on the phase transition temperature is stronger than that of oil and alcohol. From the concentrated system results it appears that type I anesthetics dehydrate the interface. The dehydration has the same effect as increasing the temperature: They reduce ethylene oxide head group hydration, allowing them to pack closer together within the aggregates, reducing the interfacial curvature, and thus shifting the phase transition temperatures to lower values (Figure 8a).

4.2.2. Type II Anesthetics. Type II anesthetics have the opposite effect to oil and alcohol, Figure 8b, increasing the phase transition temperature. Type II anesthetics carry localized charges. The charged part of the molecule associates with the base of the head group region, affecting the surface curvature. The L_α to L_3 topological transition has a zero mean bilayer interfacial curvature; however the monolayer curvature becomes negative. To minimize the electrostatic interaction between the molecules, type II anesthetics microsegregate to interfacial

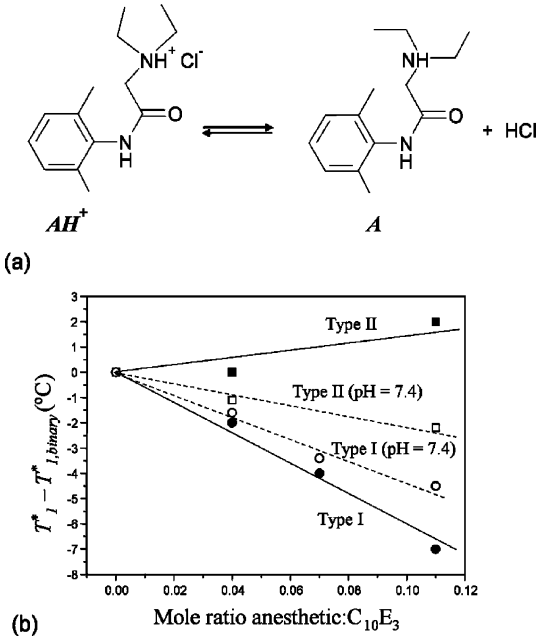

Figure 10. (a) Protonated and deprotonated forms of lidocaine. (b) Effect of lidocaine base and lidocaine hydrochloride on the L_α to $L_\alpha + L_3$ phase transition in the $C_{10}E_3$/water system by plotting the reduced temperature $T_1^* - T_{1,\text{binary}}^*$ against the anesthetic mole ratio for buffered and unbuffered solutions. Symbols are type I lidocaine base unbuffered (●) and buffered to pH = 7.4 (○) and type II lidocaine hydrochloride unbuffered (■) and buffered to pH = 7.4 (□).

regions with the most positive curvature, and thus they tend to stabilize the L_α phase and move the L_α to L_3 topological transition to a higher temperature. The effect of type II anesthetics on the surface curvature is weaker in the dilute system since only a smaller fraction of them will be associated with the interfacial region. Most of the type II anesthetic molecules reside in a water-rich environment, because of their high solubility in water.

4.2.3. Anesthetic Addition in a Buffered Solution. Buffering the pH to the physiological value of 7.4 causes all six anesthetics to shift the L_α to $L_\alpha + L_3$ phase transition temperature to lower values, so that they all behave like type I anesthetics in the $C_{10}E_3/^2H_2O$ system (Figure 8b).

The pK_a values for all of the anesthetics are in the same range p$K_a \cong 7.5-7.9$. When anesthetics are added to the $C_{10}E_3$/0.1 M PBS system, there will be a balance of protonated and deprotonated forms of the anesthetic within the sample. This is illustrated by the local anesthetics, lidocaine base (type I) and lidocaine hydrochloride (type II), Figure 10a, showing that their chemical structures are similar. Figure 10b also shows the effect of lidocaine base and lidocaine hydrochloride on the L_α to $L_\alpha + L_3$ phase transition in the $C_{10}E_3$/water system by plotting the reduced temperature $T_1^* - T_{1,\text{binary}}^*$ against the anesthetic mole ratio for buffered and unbuffered solutions. Here T_1^* is the transition temperature in the system with anesthetic, while $T_{1,\text{binary}}^*$ is the transition temperature in the corresponding binary system. In the unbuffered system containing lidocaine hydrochloride there is a larger proportion of the protonated form AH^+, which on binding to the interface encourages positive curvature, stabilizes the L_α phase, and increases T_1^*. The effect of buffering the pH on the lidocaine hydrochloride is to depress the phase transition temperature with increasing anesthetic concentration.

The unbuffered lidocaine base system contains a preponderance of the A form, which binds to the interface and dehydrates the ethylene oxide head groups, causing a decrease of T_1^*. The effect of pH buffering on the lidocaine base is that while the transition temperatures are still depressed with increasing concentration, the effect is less than that in the unbuffered system. This may be explained by considering the equilibrium between the two forms of lidocaine

$$AH^+ \leftrightharpoons A + H^+ \qquad (2)$$

Aqueous solutions of lidocaine base have a pH of approximately 9, while aqueous solutions of lidocaine hydrochloride have a pH of approximately 5.5. Therefore at pH = 7.4 there is an equilibrium between the two forms of lidocaine (eq 2). In the buffered system following lidocaine hydrochloride (i.e., AH^+) addition, the equilibrium is changed since there is a larger proportion of molecules in the A form. This fraction of lidocaine molecules in the A form dehydrates the ethylene oxide head groups, reducing interfacial curvature, hence the decrease of T_1^* with increasing anesthetic concentration. The T_1^* decrease is not so pronounced as in the unbuffered system that contains only the A form, since the fraction of this form is lower than that in the unbuffered system.

When the system to which the lidocaine base (i.e., A) was added is buffered, some of the lidocaine base molecules are protonated becoming AH^+ molecules. However, since lidocaine base dehydrates, it will have the strongest effect promoting a decrease in T^* with anesthetic concentrations, hence the lower temperature transition from the L_α to the L_3 phase (Figure 10b).

Figure 10b shows that the two lines that move toward each other represent the result of buffering the pH after the addition of lidocaine base (i.e., A form) in one case and lidocaine hydrochloride (i.e., AH^+ form) in the other case. The difference between the two lines is due to the different proportions of each form in the two systems.

Type I anesthetics promote dehydration, reducing T_1^* and thus reducing the interfacial curvature, while type II anesthetics, since they carry localized charge, favor a higher interfacial curvature to minimize the proximity of their molecules to each other, increasing T_1^*. The results show that at high dilution dehydration is the dominant effect and that when the system is buffered to physiological levels all anesthetics tend to lower the T_1^* and promote flatter interfaces.

5. Conclusion

All six anesthetic molecules investigated have a strong influence on the interfacial curvature of the two nonionic surfactant systems investigated here whether in concentrated or dilute solution. These changes arise from the binding of the anesthetic molecules to the interfacial region of the surfactant systems. Their effects classify the anesthetics into two types. Type I anesthetics (halothane, sodium thiopental, and lidocaine base form) dehydrate the ethylene oxide head groups and cause a decrease in interfacial curvature ($Mh_1(0)$ to L_α or L_α to L_3). Conversely, type II anesthetics (prilocaine hydrochloride, ketamine hydrochloride, and lidocaine hydrochloride), all of which carry a charge, tend to stabilize positive curvature in unbuffered solutions and cause an increase in interfacial curvature (L_α to $Mh_1(0)$ or L_3 to L_α). In solution buffered to physiological conditions of pH = 7.4 the two types become similar in behavior, both behaving like type I anesthetics and encouraging a decrease in interfacial curvature, although the effect is much less pronounced in type II anesthetics than in type I anesthetics (Figure 10b). It would seem that while these anesthetics do not themselves generate transmembrane pores their ability to

encourage a decrease in surface curvature may cause the switching of transmembrane channels in the more complex environment of biological membranes.

Acknowledgment. M.B. thanks the University of Central Lancashire for a research studentship. We thank Professor W. Winlow for useful discussions.

References and Notes

(1) Eckenhoff, R. G. *Mol. Interventions* **2001**, *1*, 258−268.
(2) Franks, N. P.; Lieb, W. R. *Nature* **1978**, *274*, 339−342.
(3) Franks, N. P.; Lieb, W. R. *J. Mol. Biol.* **1979**, *133*, 469−500.
(4) Brown, D. A.; London, E. *J. Biol. Chem.* **2000**, *275*, 17221−17224.
(5) Franks, N. P.; Jenkins, A.; Conti, E.; Lieb, W. R.; Brick, P. *Biophys. J.* **1998**, *75*, 2205−2211.
(6) Bhattacharya, A. A.; Curry, S.; Franks, N. P. *J. Mol. Biol.* **2000**, *275*, 38731−38738.
(7) Schoenborn, B. P. *Nature* **1967**, *214*, 1120−1122.
(8) Sachsenheimer, W.; Pai, E. F.; Schulz, G. E.; Schirmer, R. H. *FEBS Lett.* **1977**, *79*, 310−312.
(9) Miller, K. W. *Br. J. Anaesth.* **2002**, *89*, 17−31.
(10) Metcalfe, J. C.; Hoult, J. R. S. In *Molecular Mechanisms in General Anaesthesia*; Halsey, M. J., Millar, R. A., Sutton, J. A., Eds.; Churchill Livingstone: New York, 1974; pp 145−162.
(11) Lee, A. G. *Nature* **1976**, *262*, 545−548.
(12) Cafiso, D. S. *Toxicol. Lett.* **1998**, *100*−*101*, 431−439.
(13) Cantor, R. S. *Biophys. J.* **2001**, *80*, 2284−2297.
(14) Trudell, J. R.; Bertaccini, E. *Br. J. Anaesth.* **2002**, *89*, 32−40.
(15) Campagna, J. A.; Miller, K. W.; Forman, S. A. *N. Engl. J. Med.* **2003**, *349*, 910.
(16) Bach, D.; Borochov, N.; Wachtel, E. *Chem. Phys. Lipids* **2004**, *130*, 99−107.
(17) Pickholz, M.; Saiz, L.; Klein, M. L. *Biophys. J.* **2005**, *88*, 1524−1534.
(18) Franks, N. P.; Lieb, W. R. *Nature* **1997**, *389*, 334−335.
(19) Engelke, M.; Jessel, R.; Wiechmann, A.; Diehl, H. A. *Biophys. Chem.* **1997**, *67*, 127−138.
(20) Jorgensen, K.; Ipsen, J. H.; Mouritsen, O. G.; Zuckermann, M. J. *Chem. Phys. Lipids* **1993**, *65*, 205−216.
(21) Ueda, I. In *Drug and Anesthetic Effects on Membrane Structure and Function*; Aloia, R. C., Curtain, C. C., Gordon, L. M., Eds.; Wiley-Liss: New York, 1991; pp 15−33.
(22) Ueda, I.; Yoshida, T. *Chem. Phys. Lipids* **1999**, *101*, 65−79.
(23) Yoshino, A.; Yoshida, T.; Okabayashi, H.; Kamaya, H.; Ueda, I. *J. Colloid Interface Sci.* **1998**, *198*, 319−322.
(24) Engström, S.; Engström, L. *Int. J. Pharm.* **1992**, *79*, 113−122.
(25) Hyde, S.; Andersson, S.; Larsson, K.; Blum, Z.; Landh, T.; Lidin, S.; Ninham, B. *The Language of Shape: The Role of Curvature in Condensed Matter—Physics, Chemistry, and Biology*; Elsevier: New York, 1997.
(26) Qazzaz, M. M.; Winlow, W. *Acta Biol. Hung.* **1999**, *50*, 199−213.
(27) Holmes, M. C. *Curr. Opin. Colloid Interface Sci.* **1998**, *3*, 485−492.
(28) Epand, R. F.; Martinou, J. C.; Fornallaz-Mulhauser, M.; Hughes, D. W.; Epand, R. M. *J. Biol. Chem.* **2002**, *277*, 32632−32639.
(29) Leaver, M. S.; Fogden, A.; Holmes, M. C.; Fairhurst, C. E. *Langmuir* **2001**, *17*, 35−46.
(30) Puntambekar, S.; Holmes, M. C.; Leaver, M. S. *Liq. Cryst.* **2000**, *27*, 743−747.
(31) Fairhurst, C. E.; Fuller, S.; Gray, J.; Holmes, M. C.; Tiddy, G. J. T. In *Handbook of Liquid Crystals*; Demus, D., Gray, G. W., Goodby, J. W., Spiess, H. W., Vill, V., Eds.; Wiley-VCH: Weinheim, Germany, 1998; pp 341−392.
(32) Baciu, M.; Olsson, U.; Leaver, M. S.; Holmes, M. C. *J. Phys. Chem. B* **2006**, *110*, 8184−8187.
(33) Holmes, M. C.; Leaver, M. S. In *Bicontinuous Liquid Crystals*; Lynch, M. L., Spicer, P. T., Eds.; Taylor & Francis Group/CRC Press: Boca Raton, FL, 2005; pp 15−39.
(34) Fairhurst, C. E.; Holmes, M. C.; Leaver, M. S. *Langmuir* **1997**, *13*, 4964−4975.
(35) Funari, S. S.; Holmes, M. C.; Tiddy, G. J. T. *J. Phys. Chem.* **1994**, *98*, 3015−3023.
(36) Le, T. D.; Olsson, U.; Mortensen, K. *Physica B* **2000**, *276*, 379−380.
(37) Anderson, D. M.; Wennerström, H.; Olsson, U. *J. Phys. Chem.* **1989**, *93*, 4243−4253.
(38) Rendall, K.; Tiddy, G. J. T. *J. Chem. Soc., Faraday Trans. 1* **1984**, *80*, 3339−3357.
(39) Rendall, K.; Tiddy, G. J. T.; Trevethan, M. A. *J. Chem. Soc., Faraday Trans. 1* **1983**, *79*, 637−649.
(40) Burgoyne, J.; Holmes, M. C.; Tiddy, G. J. T. *J. Phys. Chem.* **1995**, *99*, 6054−6063.
(41) Fogden, A. S.; Stenluka, M.; Fairhurst, C. E.; Holmes, M. C.; Leaver, M. S. *Prog. Colloid Polym. Sci.* **1998**, *108*, 129−138.
(42) Mitchell, D. J.; Tiddy, G. J. T.; Waring, L.; Bostock, T.; Mcdonald, M. P. *J. Chem. Soc., Faraday Trans. 1* **1983**, *79*, 975−1000.
(43) Hendrikx, Y.; Charvolin, J.; Rawiso, M. *J. Colloid Interface Sci.* **1984**, *100*, 597−600.
(44) Narahashi, T.; Frazier, D. T.; Yamada, M. *J. Pharm. Exp. Ther.* **1970**, *171*, 32−44.
(45) Frazier, D. T.; Narahashi, T.; Yamada, M. *J. Pharm. Exp. Ther.* **1970**, *171*, 45−51.
(46) Cahalan, M. D.; Almers, W. *Biophys. J.* **1979**, *27*, 39−55.
(47) Strichartz, G. R. *J. Gen. Physiol.* **1973**, *62*, 37−57.